

Bis(κ N-DABCO) Magnesium(II) *Meso*-arylporphyrin: Characterization, DFT Calculations, Catalytic Degradation of Rhodamine B Dye and Inhibiting Activity of the COVID-19 Virus and Oxidase enzymes using Molecular Docking Study

Taissir Fradi ^a, Olfa Noureddine ^b, Azhar Kechiche ^a, Mohhieddine Guergueb ^a, Florian Molton ^c, Frédérique Loiseau ^c, Thierry Roisnel ^d, Ilona Turowska-Tyrk ^e, Habib Nasri ^{a,*}

^a University of Monastir, Laboratory of Physical Chemistry of Material (LR01/ES/19), Monastir, Avenue de L 'environnement, 5019 Monastir, Tunisia.

^b University of Monastir, Laboratory of Quantum and Statistical Physics (LR18ES18), Faculty of Sciences, Monastir, 5079, Tunisia

^c Département de Chimie Moléculaire, Université Grenoble Alpes, 301 rue de la Chimie, CS 40700, Cedex 9, Grenoble 38058, France

^d Institute of Chemical Sciences of Rennes, UMR 6226, University of Rennes 1, Beaulieu Campus, Rennes 35042, France.

^e Faculty of Chemistry, Wrocław University of Science and Technology, Wybrzeże Wyspiańskiego 27, Wrocław 50-370, Poland.

Contents

1. Mass spectrometry data of complex 1	2
2. Photophysical properties of complex 1	3
3. X-ray Molecular structure of 1	5
4. Hirshfeld analysis	6
5. Computational calculations	7
6. Oxidative degradation	10
7. Oxidative degradation of RhB dye using complex 1	11

1. Mass spectrometry data of complex 1

Table S1. Some attributed fragments of complex **1** from the MS ESI experiments recorded in negative and positive ion modes.

Fragment formula	Formula	m/z (calcd.)	m/z (meas.)
$[\text{Mg}(\text{TClPP})+3\text{H}]^{3+}$	$\text{C}_{44}\text{H}_{26}\text{Cl}_4\text{MgN}_4$	775.08	775.49
$[\text{Mg}(\text{TClPP})(\text{DABCO})+2\text{H}]^{2+}$	$\text{C}_{50}\text{H}_{38}\text{Cl}_4\text{MgN}_6$	886.18	886.16

2. Photophysical properties of complex 1

Table S2. Photophysical data of complex **1** and several related magnesium(II) metalloporphyrins. Measurements were recorded in dichloromethane at room temperature.

Complex	UV/Vis			Fluorescence		ϕ_f	τ_f	Ref.			
	λ_{max} (nm)			λ_{max} (nm)							
	Soret	Q(1,0)	Q(0,0)	Q(0,0)	Q(0,1)						
<i>Free base meso-arylporphyrins</i>											
H ₂ TTP ^a	420	516, 552, 594, 640		657	721	0.092	7.90	[40,41]			
H ₂ TPP ^b	418	515, 549, 591, 691		653	722	0.12	9.60	[42]			
H ₂ TMPP ^c	423	521, 558, 597, 650		656	719	0.082	7.20	[43]			
H ₂ TClPP		418(5.49) 515(4.20), 550(427), 549(3.78), 647(3.45)		652	714	0.089	7.72	t.w.			
H ₂ TBrPP ^d	419	515 549 590 648		654	720	0.054	-	[44]			
<i>Tetracoordinate Magnesium(II) meso-arylporphyrins</i>											
[Mg(TPP)] ^b	424	563,	603	608	661	0.150	-	[45]			
[Mg(TBrPP)] ^d	426	563	603	612	660	0.020	-	[44,36]			
[Mg(TClPP)]	429(5.77)	567(4.60)	607(4.52)	615	670	0.18	6.3	t.w.			
<i>Pentacoordinate Magnesium(II) meso-arylporphyrins</i>											
[Mg(TClPP)(DMAP)]	432(5.70)	570(4.69)	609(4.39)	608	659	0.16	5.0	[23]			
[Mg(TBrPP)(HIm)] ^d	429	567	607	613	662	0.024	-	[44]			
[K(222)][Mg(TPP)(N ₃)] ⁴²⁶		564	604	609	663	0.10	3.7	[45]			
[K(222)][Mg(TPP)(NCO)]	425	564	602	609	664	0.18	3.8	[45]			
<i>Hexacoordinate Magnesium(II) meso-arylporphyrins</i>											
{[Mg(TPP)(4,4'-dipy) ₂] } _n ^b	431(5.86)	570(460)	610(4.39)	617	575	-	-	[46]			

[Mg(TPBP)(4,4'-bpy) ₂] ^e	430(6.04)	571(5.08)	614(5.00)	611	665	0.06	-	[47]
[Mg(TPP)(THF) ₂] ^b	426(5.75)	564(4.25)	604(3.95)	609	660	0.16	8.9	[48]
[Mg(TPP)(HMTA) ₂] ^b	434(6.22)	575(4.97)	617(4.98)	620	665	0.14	4.7	[49]
[Mg(TPBP)(HMTA) ₂] ^e	535(5.88)	576(4.33)	617(4.40)	611	666	0.06	-	[36]
[Mg(TPBP)(DABCO) ₂] ^e	429(5.78)	565(4.44)	605(4.20)	612	666	0.07	-	[36]
[Mg(TTP)(DMAP) ₂] ^a	427	566	606	611	665	0.13	5.0	[22]
[Mg(TTP)(4-pypo) ₂] ^a	427	565	606	611	663	0.13	4.6	[38]
[Mg(TClPP)(DABCO) ₂] (1)	430(5.33)	567(4.11)	606(3.96)	609	664	0.06	5.09	t.w.

^a: TTP = *meso*-tetra(*para*-tolyl)porphyrinate, ^b: TPP = *meso*-tetraphenylporphyrinate, ^c: TMPP = *meso*-tetra(*para*-methoxyphenyl)porphyrinate, ^d: TBrPP = *meso*-tetra(*para*-bromophenyl)porphyrinate, ^e: TPBP = *meso*-tetrakis[4(benzoyloxy)phenyl]porphinate.

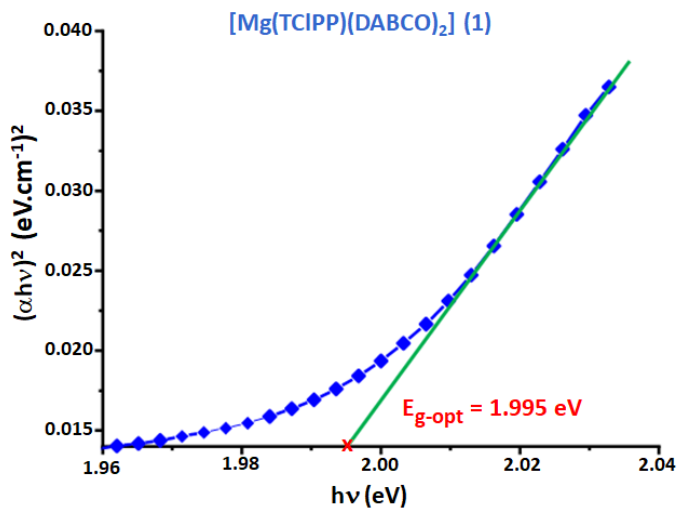


Figure S1. Plot of $(\alpha h\nu)^2$ versus the photon energy ($h\nu$) of complex **1**. $h\nu$ is the incident photon energy and α is the absorption coefficient.

3. X-ray molecular structure of **1**

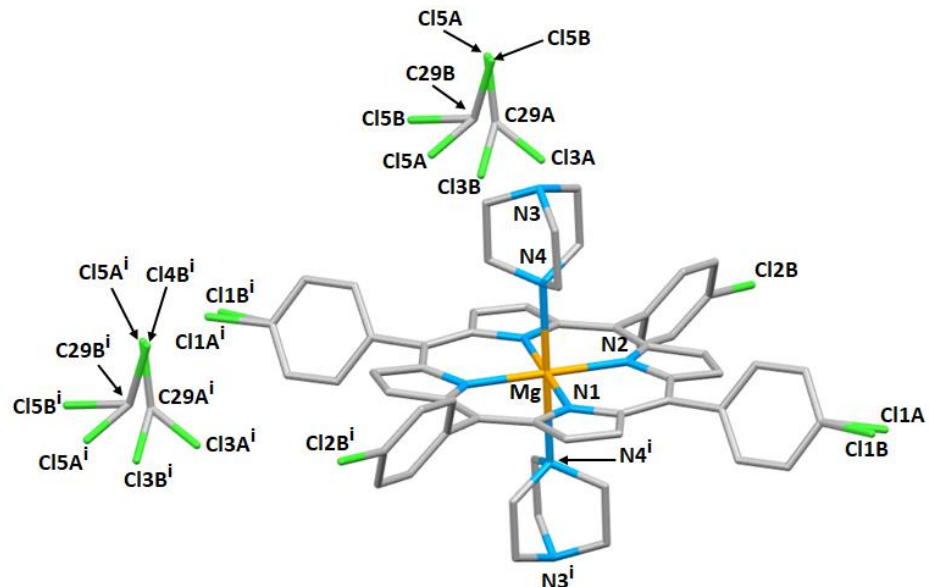


Figure S2. Drawing showing the structure of complex **1** with the Formula $[\text{Mg}(\text{TClPP})(\text{DABCO})_2] \cdot 2\text{CHCl}_3$.

Table S3. Selected intermolecular interactions for complex 1.

D–H \cdots A ^a	Symmetry of A	D \cdots A (Å)	D–H \cdots A (°)
C2-H2...Cl3B	x-1,y,z	3.468(5)	138
C9-H9...Cl1A	1/2-x,y-1/2,1/2-z	3.344(3)	123

^a: D = donor atom and A = acceptor atom.

4. Hirshfeld analysis of complex 1

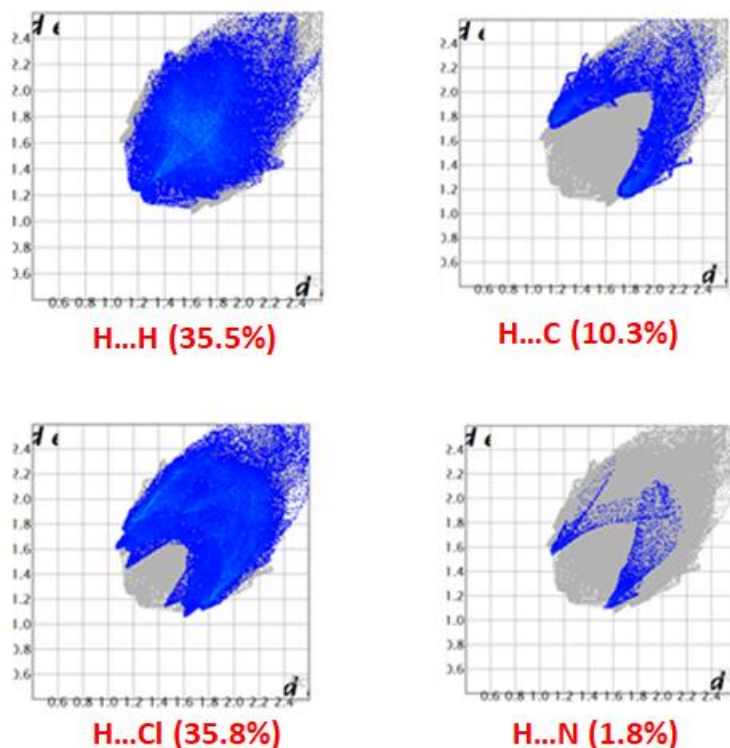


Figure S3. Fingerprint plots of complex 1.

5. Computational calculations

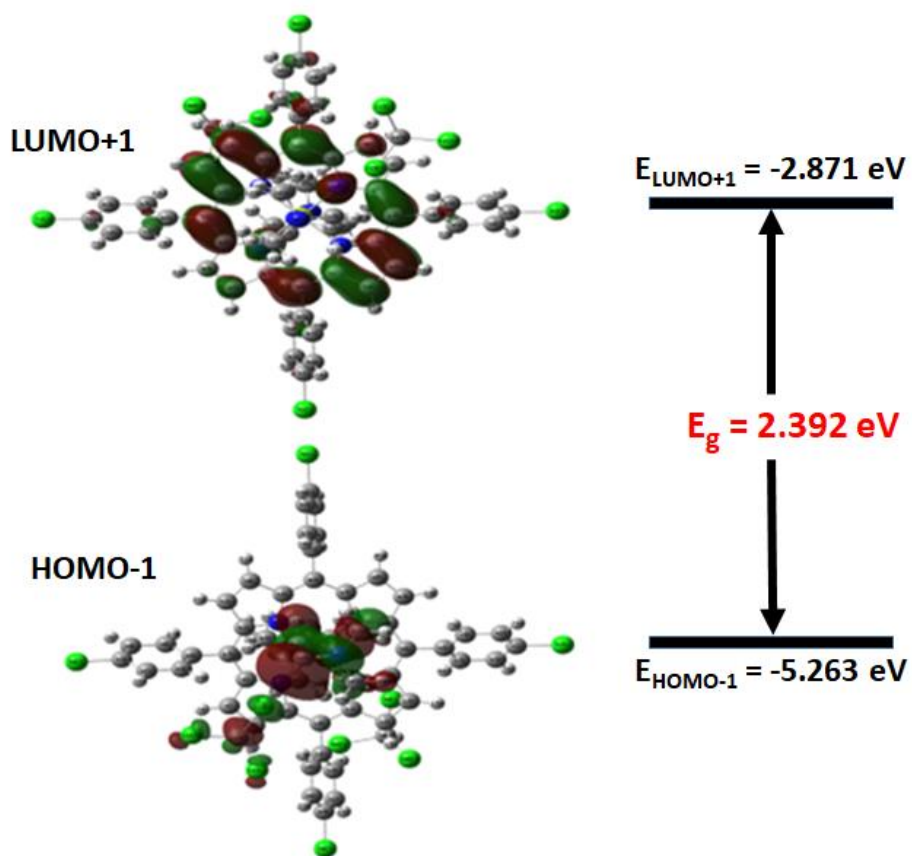


Figure S4. HOMO and LUMO frontier orbitals of complex 1 calculated in the chloroform solvent.

Table S4. Theoretical and experimental bond lengths (\AA) and angles ($^\circ$) of $[\text{Mg}(\text{TCIPP})(\text{DABCO})_2]$.

Atom1	Atom2	Experimental value	Theoretical value B3LYP/LANL2DZ method
Mg	N1	2.081	2.052
Mg	N2	2.065	2.095
Mg	N1	2.081	2.085
Mg	N2	2.065	2.100
Mg	N4	2.474	2.330
N1	C1	1.368(2)	1.376

N1	C4	1.369(3)	1.345
N2	C6	1.369(3)	1.345
N2	C8	1.369(2)	1.347
C1	C2	1.449(3)	1.446
C1	C10	1.410(3)	1.420
C2	H2	0.930	0.933
C2	C3	1.353(3)	1.350
C3	H3	0.931	0.931
C3	C4	1.446(3)	1.450
C4	C5	1.415(3)	1.423
C5	C6	1.413(3)	1.408
C5	C11	1.492(3)	1.500
C6	C7	1.448(3)	1.452
C7	H7	0.929	0.935
C7	C9	1.348(3)	1.351
C8	C9	1.448(3)	1.457
C8	C10	1.411(3)	1.423
C9	H9	0.930	0.941
C10	C17	1.500(3)	1.511
C10	C8	1.411(3)	1.417
C11	C12	1.401(3)	1.399
C11	C16	1.396(3)	1.394
C12	H12	0.929	0.932
C12	C13	1.383(3)	1.381
C13	H13	0.930	0.937
C13	C14	1.377(3)	1.380
C14	C15	1.387(3)	1.391
C14	Cl1A	1.745(3)	1.747
C15	H15	0.930	0.932
C15	C16	1.388(3)	1.390
C16	H16	0.930	0.935
C17	C18	1.393(3)	1.398
C17	C22	1.390(3)	1.392
C18	H18	0.930	0.935
C18	C19	1.390(3)	1.396
C19	H19	0.931	0.938
C19	C20	1.378(3)	1.388
C20	C21	1.375(4)	1.376
C20	Cl2B	1.745(2)	1.751
C21	H21	0.929	0.915
C21	C22	1.392(3)	1.388
C22	H22	0.930	0.930
N1	C1	1.368(2)	1.370
N1	C4	1.369(3)	1.373
N2	C6	1.369(3)	1.361

N2	C8	1.369(2)	1.375
C1	C2	1.449(3)	1.450
C1	C10	1.410(3)	1.418
C2	H2	0.930	0.944
C2	C3	1.353(3)	1.356
C3	H3	0.931	0.930
C3	C4	1.446(3)	1.449
C4	C5	1.415(3)	1.420
C5	C6	1.413(3)	1.419
C5	C11	1.492(3)	1.488
C6	C7	1.448(3)	1.441
C7	H7	0.929	0.929
C7	C9	1.348(3)	1.349
C8	C9	1.448(3)	1.453
C9	H9	0.930	0.934
C10	C17	1.500(3)	1.510
C11	C12	1.401(3)	1.411
C11	C16	1.396(3)	1.399
C12	H12	0.929	0.935
C12	C13	1.383(3)	1.387
C13	H13	0.930	0.935
C13	C14	1.377(3)	1.380
C14	C15	1.387(3)	1.390
C14	Cl1A	1.745(3)	1.747
C15	H15	0.930	0.936
C15	C16	1.388(3)	1.390
C16	H16	0.930	0.933
C17	C18	1.393(3)	1.399
C17	C22	1.390(3)	1.392
C18	H18	0.930	0.931
C18	C19	1.390(3)	1.390
C19	H19	0.931	0.931
C19	C20	1.378(3)	1.380
C20	C21	1.375(4)	1.378
C20	Cl2B	1.745(2)	1.740
C21	H21	0.929	0.930
C21	C22	1.392(3)	1.391
C22	H22	0.930	0.933
N3	C23	1.463(4)	1.462)
N3	C26	1.457(3)	1.456
N3	C27	1.463(4)	1.461
N4	C24	1.477(3)	1.478
N4	C25	1.474(3)	1.475
N4	C28	1.472(3)	1.473
C23	H23A	0.970	0.971

C23	H23B	0.969	0.969
C23	C24	1.551(4)	1.552
C24	H24A	0.970	0.970
C24	H24B	0.969	0.970
C25	H25A	0.970	0.971
C25	H25B	0.970	0.972
C25	C26	1.547(4)	1.548
C26	H26A	0.971	0.970
C26	H26B	0.970	0.973
C27	C28	1.552(4)	1.551
C28	H28A	0.970	0.971
C28	H28B	0.970	0.970
C29A	H29A	0.979	0.980
C29A	Cl3A	1.761(4)	1.762
C29A	Cl4A	1.751(6)	1.753
C29A	Cl5A	1.761(4)	1.762

6. Docking results

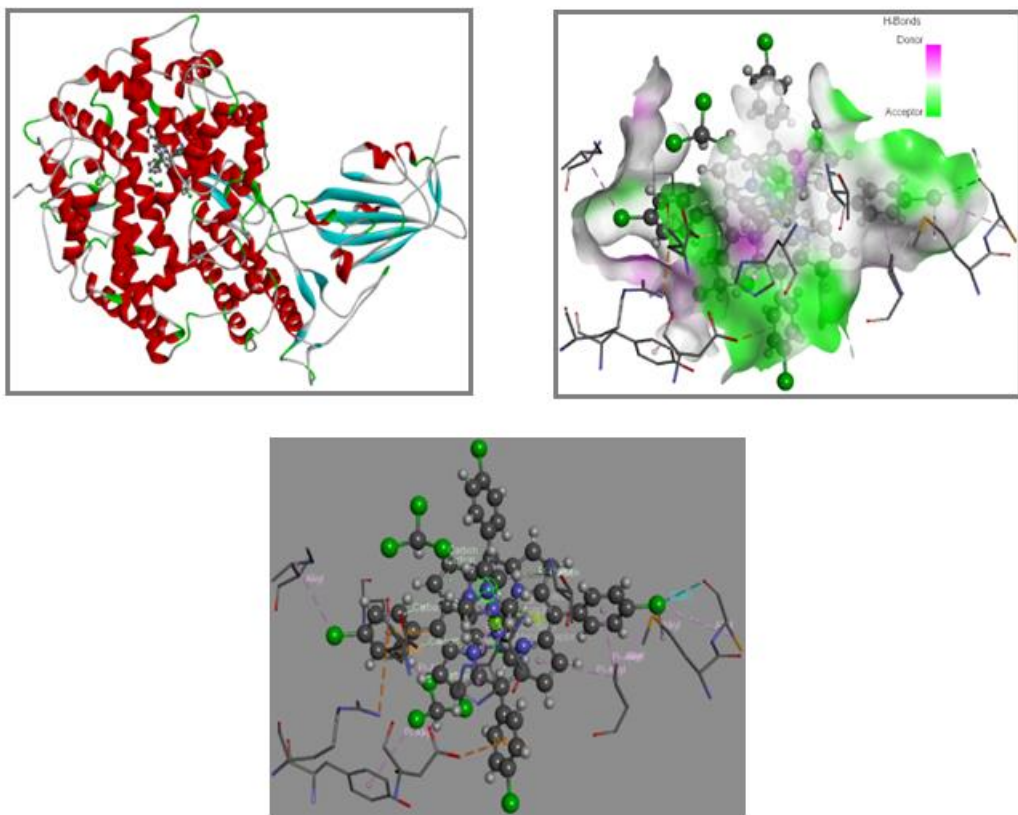


Figure S5. Docking interactions of complex 1 in the active sites of 1H4O protein.

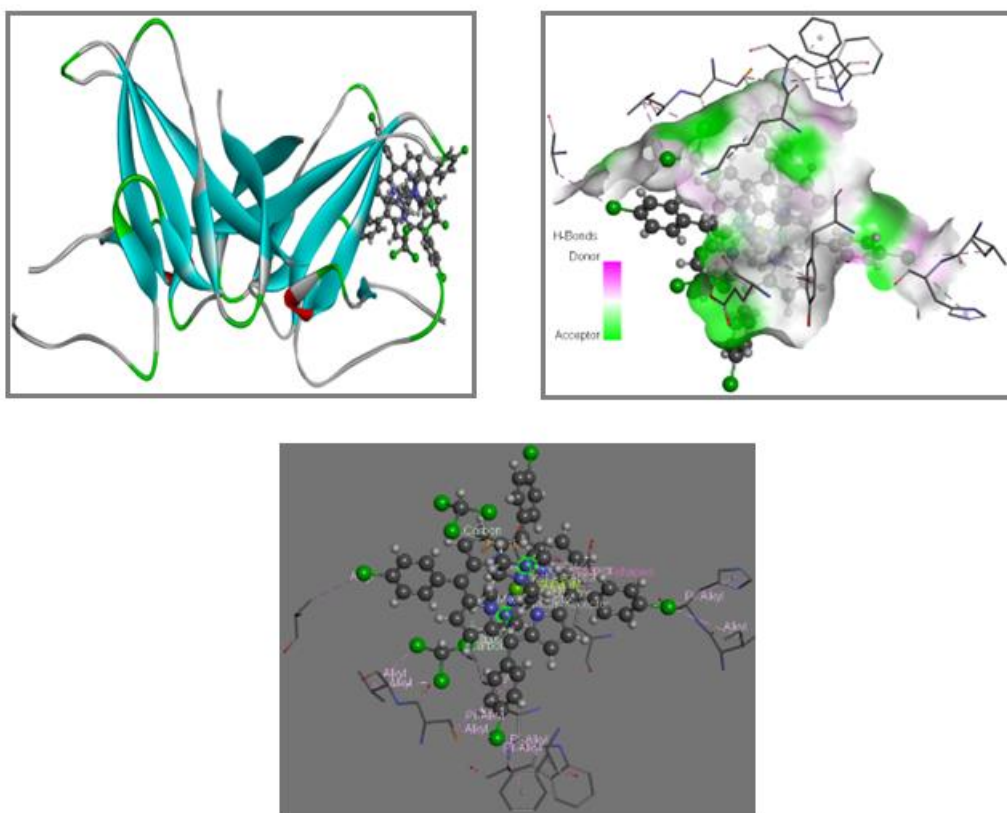


Figure S6. Orientation of complex **1** in the active sites of ORF8 receptor.

7. Oxidative degradation of RhB dye using complex **1**

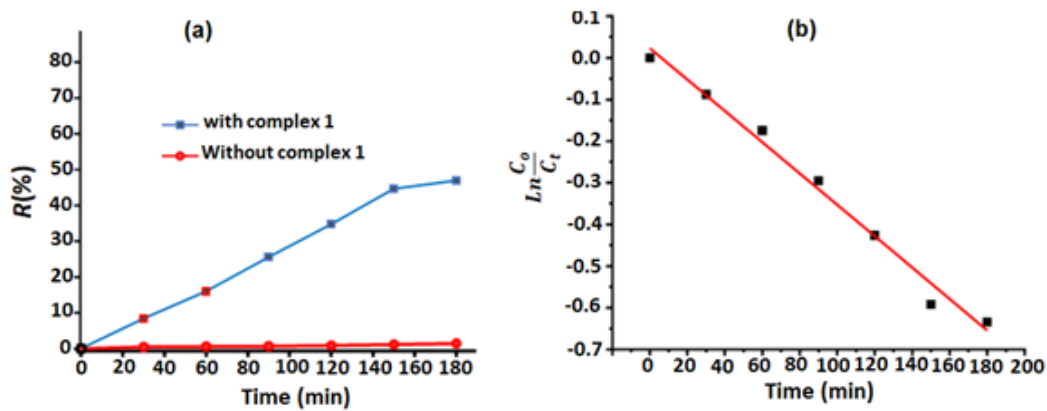


Figure S7. **(a):** Variation of the yield [$R(\%)$] as a function of time, **(b):** Variation of $\ln(C_t/C_0)$ as a function of time.

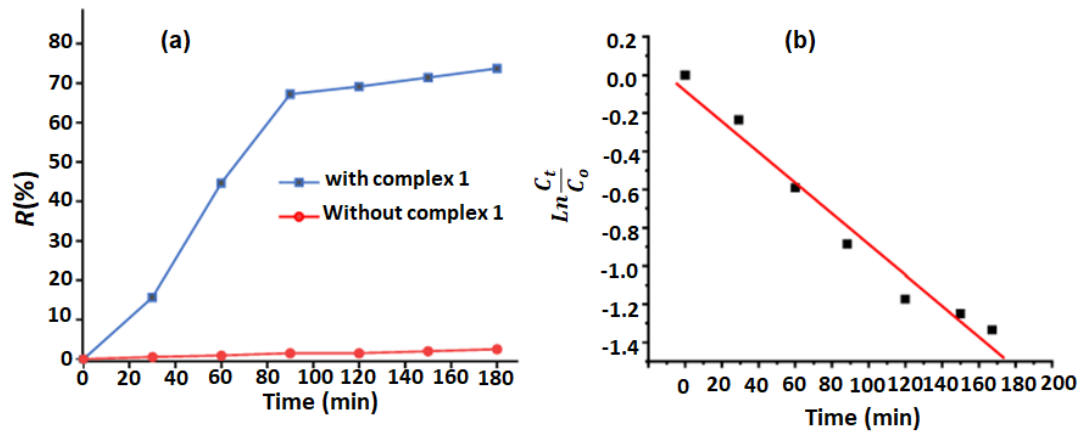


Figure S8. (a): Variation of photooxidation yield [$R(\%)$] as a function of time, (b): Variation of $\ln(C_t/C_0)$ as a function of time.